Glucolipotoxic conditions induce β-cell iron import, cytosolic ROS formation and apoptosis

Jakob Bondo Hansen[1,2,5], Laila Romagueira Bichara Dos Santos[3], Ying Liu[2], Kacey J Prentice[2], Frederik Teudt[1], Morten Tonnesen[4], Jean-Christophe Jonas[3], Michael B Wheeler[2], Thomas Mandrup-Poulsen[1]

1: University of Copenhagen, Dept. of Biomedical Sciences, Copenhagen, DK-2200, Denmark.
2: University of Toronto, Dept. of Physiology, Toronto, ON, M5S 1A8, Canada.
3: Université Catholique de Louvain, Institute of Experimental and Clinical Research, Pole of Endocrinology, Diabetes and Nutrition, Brussels, 1200, Belgium.
4: Novo Nordisk, Dept. of Diabetes Complications Biology & Pharmacology, Novo Nordisk Park, Måløv, DK-2760, Denmark.
5: Corresponding author, jakobha@sund.ku.dk.

Short title: Iron uptake mediates β-cell glucolipotoxicity

Keywords: intrinsic death pathway, diabetes, insulin secretion, gluco-lipotoxicity.

Abstract

Type 2 diabetes (T2D) arises when the pancreatic beta-cell fails to compensate for increased insulin needs due to insulin resistance. Glucolipotoxicity has been proposed to induce beta-cell dysfunction in T2D by formation of reactive oxygen species (ROS). Here we examined if modelling glucolipotoxic conditions by high glucose-high free fatty acid (FFA) exposure (GLT) regulate beta-cell iron transport, thereby increasing the cytosolic labile iron pool and iron-catalyzed ROS formation. We show that GLT - induced ROS production is regulated by an increased labile iron pool (LIP) associated with elevated expression of genes regulating iron import. Using pharmacological and transgenic approaches, we show that iron reduction and decreased iron import protects from GLT-induced ROS production, prevents impairment of the mitochondrial membrane potential, and inhibits apoptosis. This study identifies a novel pathway underlying GLT-induced apoptosis involving increased iron import, generation of hydroxyl radicals from hydrogen peroxide through the Fenton reaction in the cytosolic compartment associated with dissipation of the mitochondrial membrane potential and beta cell apoptosis.

Introduction

Chronic nutritional overload is a very recent event in evolution, against which the development of cellular defense mechanisms has therefore not been advanced by selection pressure. In contrast, fluctuations in circulating substrate levels as a result of bouts of fasting and feeding have prevailed throughout human history and have selected for acute accommodations to nutritional fluxes, thereby defining the physiological regulation of metabolism. The pathophysiology of metabolic disorders is thus in part characterized by the adverse effects of inappropriate handling of nutritional overload, and in part by aberrant and chronic activation of normal metabolic pathways. Much is still to be learned about the molecular sensing, signaling and organelle relaying of substrate overload. Three main hypotheses have been proposed to explain the impairment of cellular replication, differentiation, function, and survival caused by increased circulating levels of FFAs and glucose now by many referred to as gluco-lipotoxicity (GLT) (Muoio and Newgard 2008): oxidative stress mediated by excess generation of reactive oxygen intermediates (ROS); lipid partitioning, i.e. redirection of FFA metabolism from beta-oxidation to build-up of toxic lipid metabolites and lipid storage; and activation of low-grade inflammation. The molecular mechanisms regulating and executing the consequences of these major pathways are only partially understood.

In highly metabolically active cells such as cardiomyocytes and hepatocytes exhibiting high mitochondrial densities, the oxidative burden is typically counteracted by high mitochondrial oxidative capacity and by the expression of antioxidant enzymes (Lenzen 2017; Lenzen, et al. 1996). In spite of lower mitochondrial density, the highly metabolically active pancreatic beta-cells are uniquely sensitive to oxidative stress due to inadequate antioxidant defense (Lenzen et al. 1996).

Iron-sulfur (Fe-S) proteins in the electron transport chain (ETC) contribute to the generation of ROS from the mitochondria via the Fenton reaction (Thomas, et al. 2009) and in the cytosol via NAPDH oxidase activity (Bedard and Krause 2007). Tissue iron overload confers risk for the development of diabetes (Ellervik, et al. 2011; Ellervik, et al. 2001; Jehn, et al. 2004; Jiang, et al. 2004; Montonen, et al. 2012), and diabetes and the metabolic syndrome are associated with elevated circulating ferritin, a marker of cellular iron deposition (Ford and Cogswell 1999; Gabrielsen, et al. 2012). Additionally, human and rodent beta-cells accumulate iron in conditions of increased circulating iron, as seen in hereditary hemochromatosis and transfusional iron overload, promoting islet apoptosis, decreased islet mass and impaired insulin secretion due to increased ROS production (Cooksey, et al. 2004; Lu and Hayashi 1994; Lu, et al. 1991). These clinical observations confirm that the beta-cell is particularly vulnerable to aberrant intracellular iron accumulation.

It is not known if GLT plays a causal role in enhancing beta-cell iron transport, thereby leading to excess ROS formation, beta-cell dysfunction and apoptosis. Therefore, we investigated this important science gap of considerable translational importance for the development of novel antidiabetic therapies targeting beta-cell iron handling.

Materials and Methods

Animal care

Mice were housed with access to water and food *ad libitum*, in a 12 hr light/dark cycle (Hansen, et al. 2012) (Supplemental Materials and Methods).

All the protocols were approved by the animal care committee of the University of Toronto or Danish Animal Inspectorate.

Islet isolation

Islets were isolated after collagenase digestion and hand-picked (Supplemental Materials and Methods).

Cell culture and treatment

MIN6 cells were cultured in DMEM (Gibco, Hvidovre, DK) containing 4.5 g/L glucose, 10% foetal bovine serum (FBS, Gibco, Hvidovre, DK), 0.1% penicillin and streptomycin, and 50 μmol/L beta-mercaptoethanol (Gibco, Hvidovre, DK).

Isolated islets were cultured in RPMI 1640 supplemented with 10% FBS and 0.1% penicillin and streptomycin at 37°C with 5% CO_2.

For GLT treatment, culture medium was supplemented with or without endotoxin-free glucose and/or palmitate +/- oleate (both Invitrogen, Nærum, Denmark) dissolved in 80% ethanol. Fatty acids were conjugated to BSA for at least 4 hours at 37 °C in a molar ratio of 3:1 in culture medium prior to use, and the final concentrations were: palmitate (400 μM), combination of fatty acids palmitate (200 μM) and oleate (200 μM) and glucose 30 mM. Islets and MIN6 cells were treated with up to 72 hours and human islets for 24 hours. Culture medium supplemented with BSA and ethanol was used as control for GLT.

IL-1β (150 pg/mL) (BD Bioscience Pharmingen, San Diego, CA, USA) and IFN-γ (5 ng/mL) (R&D Systems, Bad Nauheim, Germany) exposure was performed for 24 hours.

The iron chelator desferroxamine (DFO) (Sigma, Brøndby, Denmark) was dissolved in water and deferasirox (D-sirox) (Santa Cruz Biotechnology, Heidelberg, Germany) diluted in DMSO and added directly to the culture medium (See also Supplemental Materials and Methods).

Glucose-stimulated insulin secretion perifusion and total islet insulin content: Basal insulin secretion was established by pre-incubating islets or MIN6 cells for at least one

hour in 3 mM glucose KRB. For stimulation, islets or MIN6 cell were incubated in KRB with the given concentrations of glucose for 30 minutes. KCl-induced insulin secretion was performed with 16.7 mM glucose and 30 mM KCl for 30 minutes. After GSIS experiments islets were lysed in ethanol-HCl at -20°C for at least 24 hours. Lysates were dried in a vacuum centrifuge, pellets were dissolved in ultra-pure water, and DNA was measured by spectrophotometry using NanoDrop 2000 (Thermo Fisher, DK).

Islet perifusion: Fifty islets from littermates were preincubated in KRB (3 mM Glc) for two hours in KRB prior to perifusion, and then perifused at a flow rate of 1 mL per minute (Hansen et al., 2012). Total islet insulin was extracted from 10-20 islets lysed in ethanol-HCl at -20°C for at least 24 hours. Insulin was measured using an insulin homogeneous time resolved fluorescence (HTRF) kit according to manufacturer's protocol (Cisbio, Codolet, France), or insulin ELISA (Kekow et al., 1988).

Calcein assay

Islets were incubated in imaging buffer with 0.25 μM calcein-AM (Molecular Probes, Nærum, Denmark) for 1 hour. Fluorescence was detected and analyzed as described (Hansen et al. 2012) and Supplemental Materials and Methods.Total islet calcein loading was measured after chelation with 0.015 mM D-Sirox, and changes in LIP was calculated as difference between total calcein load and quenched calcein fluorescence.

Quantitative PCR

RNA was extracted using RNeasy Mini Kit (Qiagen, Copenhagen, DK), and RNA was measured using NanoDrop 2000 (Thermo Fisher, DK). cDNA was synthesized using

SuperScript II Reverse Transcriptase (Sigma, Brøndby, DK), run with SybrGreen (Applied Biosystems, Nærum, DK), and analyzed on ViiA7 Real-Time PCR System (Applied Biosystems, Nærum, DK). Primers were purchased from TagCopenhagen (Copenhagen, DK) (Supplemental Materials and Methods).

Mitochondrial membrane potential and HIF1a translocation

Mitochondrial membrane potential and HIF1a translocation were measured in whole islets as previously described (Chan, et al. 2001; Cheng, et al. 2010) (Supplemental Materials and Methods). In brief, islets were loaded with Rhodamine123 (Rhod123; Molecular Probes, Nærum, Denmark) (2.5 mg/mL) for 10 min in imaging buffer and the increase in mitochondrial membrane potential was measured as quenching of Rhod123 fluorescence. Fluorescence was recorded and analysed as described in Supplemental Materials and Methods.

Apoptosis assay

Twenty-five islets per condition in duplicates were used for apoptosis assay. Apoptosis was detected using Roche Cell Death Detection ELISA (Roche, Hvidovre, DK) according to the manufacturer's protocol.

ROS

Islets were loaded with CM-H2DCFDA (Molecular Probes, Nærum, Denmark) (10 μM) for 45 minutes in imaging buffer, washed once and ROS was detected on Flex Station 3 as described (Friberg, et al. 2010) and Supplemental Materials and Methods).

Quantification of cytosolic and mitochondrial thiol oxidation

Islets were cultured, in batches of 10 at different glucose concentrations and/or palmitate with or without DFO (0.1 mM), infected with adenovirus coding mito-roGFP1 or cyto-roGFP1 and transferred to a perifusion chamber in inverted microscope and fluorescence was measured every 30 s. After 20 min, 10 mM DTT was added to maximally reduce roGFP1, followed by 100 μM aldrithiol to maximally oxidize roGPF. The fluorescence ratio during the initial perifusion period was normalized to the ratio in DTT (set to 0%) and in aldrithiol (set to 100%). (Roma, et al. 2012) and Supplemental Materials and Methods).

Statistics

Statistics were performed using Prism (GraphPad, La Jolla, CA, USA). Student's t-test, and one- and two-way ANOVA with Bonferroni's post hoc test were used to assess significance. $p < 0.05$ was considered statistically significant.

Results

Glucolipotoxicity increases the beta-cell labile iron pool.

Islets isolated from mice fed a high fat diet (HFD) for eight weeks had significantly increased LIP compared to islets from control-fed mice (Fig. 1A). GLT exposure *in vitro* for up to 72 hours (Fig. 1B), but not palmitate alone (Fig. S1A), significantly increased the islet LIP after 48 hours compared to vehicle-treated islets. Of note, a combination of palmitate and oleate considered to a be more relevant model of glucolipotoxicity *in vivo* significantly increased the LIP in isolated human islets (Fig. 1C) to an even higher degree than the pro-inflammatory cytokines IL-1β and IFN-γ (Fig. 1D), previously shown to upregulate the iron transporter divalent metal transporter (DMT) 1 in human islets (Hansen et al., 2012).

To verify that the increase in islet LIP was beta-cell derived, we exposed insulin-producing mouse MIN6 cells to palmitate for up to 72 hours. We did not manipulate the glucose concentration in MIN6 cell experiments, since MIN6 cells are normally grown in 25 mM glucose. Palmitate significantly increased LIP in MIN6 cells after 24 hours of exposure (Fig. 1E). This increase in beta-cell LIP was associated with decreased glucose-induced insulin secretion and increased ROS production and apoptosis (Fig. S1B-D).

Next, we investigated if the GLT-mediated increase in the beta-cell LIP was associated with changes in expression of iron handling genes in MIN6 cells exposed to palmitate for up to 24 hours (Figs. 1F-G and S1E-G). Palmitate significantly increased expression of the iron import genes DMT1 and transferrin receptor (*Trfr*) after 18 and 24 hours, while the iron storage gene ferritin heavy chain (*Fth*) was transiently downregulated at 6 hours. Ferritin light chain (*Ftl*) and the iron export gene ferroportin (*Fpn*) were not regulated by palmitate exposure. Since increased ROS production has been suggested to induce beta-cell dysfunction through altered transcriptional activity (Prentice, et al. 2014), we measured the expression of the beta-cell transcription factor pancreatic and duodenal homeobox 1 (*Pdx1*). *Pdx1* was transiently downregulated after 6 hours of palmitate exposure, while insulin 1 (*Ins1*) gene expression was unaffected (Fig. S1H-I), suggesting that GLT-induced transient differences in transcriptional activity are not responsible for the observed differences in GSIS.

Iron-mediated beta-cell apoptosis is associated with an increase in cytosolic thiol oxidation

To investigate the causal role of GLT-induced increases in intracellular beta-cell LIP for apoptosis, we used the pharmacological iron chelator DFO to decrease the LIP in

islets. DFO reduced the beta-cell LIP in a concentration-dependent manner after 48 hours of treatment (Fig. 2A), without impacting absolute levels of GSIS, islet insulin content, accumulated insulin secretion or HIF1α nuclear translocation (Fig. S2A-C and data not shown). The stimulatory index of the GSIS from the iron-chelated islets was decreased as expected (Fig. S2A). The impact of the beta-cell LIP on GLT-induced apoptosis was then investigated in isolated islets exposed to vehicle or GLT for 48 hours in the presence or absence of DFO. GLT significantly increased islet apoptosis two-fold, which was completely prevented by co-treatment with DFO (Fig. 2B).

We next asked if an increase in the LIP in islets exposed to a moderate glucose concentration (G11), G11 supplemented with palmitate (G11_PA), high glucose (G30), or G30 supplemented with palmitate (G30_PA) caused an increase of ROS in the cytosol or in the mitochondria (Fig. 2C-D). We first verified that DFO did indeed reduce GLT-induced LIP in a concentration-dependent manner in MIN6 cells (Fig. S2D). Palmitate exposure for 48 hours increased thiol oxidation in the cytosol independently of iron, since DFO co-treatment did not reduce cytosolic thiol oxidation (Fig. 2C). This was consistent with the inability of palmitate alone to increase the beta-cell LIP (Fig. S1A). In contrast, high glucose in combination with palmitate increased islet cytosolic thiol oxidation, which was decreased by iron chelation using DFO (Fig. 2C). Islet mitochondrial thiol oxidation was significantly decreased by DFO at basal, G30 and G30_PA, whereas a 48 h exposure to high glucose or palmitate did not change the mitochondrial thiol oxidation (Fig. 2D).

DFO treatment protected against FFA-mediated dysfunction estimated by GSIS and KCl-induced insulin secretion in islets exposed to a combination of palmitate and oleate for 24 hours (Fig. 2E) shown above to increase human islet LIP (Fig. 1C),

Iron is required for normal mitochondrial function

Tamoxifen-inducible beta-cell specific DMT1 KO (Cre^+Flox^+) islets (Fig. S3A) had significantly decreased LIP (Fig. 3A) resulting in decreased ROS formation compared to WT (Cre^-Flox^+) islets (Fig. 3B).

Since cytosolic ROS production promotes mitochondrial superoxide generation that may impair mitochondrial function (Coughlan, et al. 2009), we next investigated the change in mitochondrial membrane potential (MMP) of isolated Cre^-Flox^+ and Cre^+Flox^+ islets upon glucose stimulation (Fig. 3C). At 3 mM glucose, Cre^+Flox^+ islets exhibited a significant hyperpolarization of the MMP compared to Cre^-Flox^+ islets, confirming that the decreased GSIS observed in Cre^+Flox^+ islets, is due to inability to increase the MMP upon high glucose exposure. The MMP of Cre^-Flox^+ and Cre^+Flox^+ islets were similar when stimulated with 20 mM glucose, as well as when the mitochondria were completely depolarized using NaN_3.

DMT1 KO protects from GLT-induced islet apoptosis associated with decreased ROS formation and preservation of the MMP

GLT-induced islet apoptosis was completely inhibited in Cre^+Flox^+ islets compared to Cre^-Flox^+ islets (Fig. 4A), and correlated with decreased GLT-induced ROS formation (Fig. 4B). Additionally, since lipotoxic exposure of islets promotes attraction of pro-inflammatory macrophages to the islets to facilitate islet dysfunction (Eguchi et al., 2012), we investigated islet secretion of IL-6, TNF-α and MCP-1 (Fig. S4A-F). We did not observe upregulation of the cytokines or the chemoattractant by GLT; however, DFO treatment significantly reduced the production of MCP-1. Iron chelation with DFO, but not DMT1 KO, significantly increased islet production of TNF-α, suggesting that this action is not associated with iron chelating properties of DFO.

Since $Cre^{+}Flox^{+}$ islets were completely protected from apoptosis induced by 48 hours of GLT exposure, we wanted to investigate if $Cre^{+}Flox^{+}$ islets had preserved secretory function. The stimulatory index of the GLT exposed DMT1 KO islets was significantly increased compared to GLT exposed WT islets (Fig.4C), showing that DMT1 KO in addition to protecting from GLT-induced apoptosis improves the ability of the islets to respond to glucose.

We next wanted to investigate if reduced ROS formation in $Cre^{+}Flox^{+}$ islets protected mitochondrial function by measuring islet MMP after 48 hours exposure to GLT (Fig. 4D-E). GLT did not affect the MMP at 3mM glucose in $Cre^{-}Flox^{+}$ islets; notably however, at 20 mM glucose $Cre^{-}Flox^{+}$ islets exposed to GLT had significantly decreased MMP compared to vehicle exposed $Cre^{-}Flox^{+}$ islets as measured by the area under the curve. In $Cre^{+}Flox^{+}$ islets, 48 hours exposure to GLT neither affected the MMP at 3mM glucose or the MMP at 20mM glucose compared to vehicle treated $Cre^{+}Flox^{+}$ islet, suggesting that protection from cytosolic ROS formation prevented mitochondrial damage, and subsequent impairment in MMP.

Discussion

In the present study we investigated the mechanisms of GLT-induced beta-cell ROS production and cellular dysfunction. We found that GLT specifically alters the iron metabolism in beta-cells both *in vivo* and *in vitro* resulting in apoptosis. GLT induced *Dmt1* and *Trfr* mRNA up-regulation in beta-cells, and this was associated with increased iron uptake, increased intracellular LIP, cytosolic ROS production, mitochondrial dysfunction and beta-cell apoptosis. Importantly, we observed an increase in islet LIP from islets isolated from mice fed HFD for 8 weeks, where severe

beta-cell damage is yet to occur but dysfunction is progressing. This suggests that increases in LIP and ROS formation might precede apoptosis *in vivo*.

Our work is in line with previously published findings by ourselves and others, where decreased dietary iron or decreased iron uptake protects beta-cells from HFD-induced dysfunction (Cooksey, et al. 2010; Hansen et al. 2012). However, this observation was recently challenged in a study claiming that palmitate-mediated beta-cell apoptosis is mediated through a *reduction* in LIP and that DFO promotes beta-cell apoptosis (Jung, et al. 2015). Because DFO is a potent iron chelator and iron is an absolute growth requirement for insulin-producing cells (Nielsen 1989), it is not surprising to us that DFO induces beta-cell apoptosis, which we have in fact demonstrated in MIN6 cells at concentrations of ≥0.1 mM (Hansen, JB; unpublished data). It is therefore important to carefully titrate iron chelators for such studies.

Dmt1 and *Trfr* are likely upregulated by JNK activation and ER stress, since 1) they contain predicted binding sites for the transcription factors AP1 and XBP1 respectively; 2) AP1 activity is increased by glucotoxicity in a beta-cell line; and 3) *Xbp1* mRNA is increased in rat islets by palmitate exposure and by palmitate and oleate exposure in human islets respectively (Cunha, et al. 2008; Maedler, et al. 2008). These observations also provide a potential mechanism for the synergistic effect of glucose and FFAs in inducing the LIP in mouse beta-cells.

From studies in hepatocytes, another highly metabolically active cell, it has been proposed that GLT-induced ROS formation is caused by physical interaction between the mitochondria and ER with release of calcium from the ER to the mitochondria, resulting in decreased mitochondrial function, increased mitochondrial ROS formation

and JNK activation (Arruda, et al. 2014). Importantly, our data suggests that GLT induces cytosolic ROS production, rather than increasing mitochondrial ROS production. This, however, does not exclude GLT-induced beta-cell ER-mitochondrial interactions via calcium signalling and mitochondrial ROS production post or prior to iron accumulation, since DFO and DMT1 have limited or no calcium affinity (Ehrnstorfer, et al. 2014; Munoz, et al. 2011).

Recently, iron uptake in metabolically unstressed human beta-cells was proposed to be carried out primarily via non-transferrin dependent iron import by the plasma membrane protein ZIP14 (solute carrier family 39 member 14, SLC39A14), independently of DMT1 and TRFR (Coffey and Knutson 2017), suggesting the existence of two distinct pathways for iron uptake. We hypothesize a physiological role for DMT1 to maintain insulin secretion by controlling the LIP and thereby the ROS levels required to fine-tune insulin-secretion driven by the stimulus-secretion coupling. Of note we found that the iron chelator DFO decreased the islet mitochondrial but not the cytosolic thiol oxidation in the absence of metabolic stress. This suggests that under normal conditions the cytosolic LIP and ROS production is minimal and their contribution to GSIS likely to be limited. In addition, it confirms previous findings that mitochondrial function and ROS production primarily contribute to GSIS (Leloup, et al. 2009), and shows the importance of iron in maintaining mitochondrial ROS production.

A caveat for the *in vivo* translation of the findings in this study is the diverse reports regarding the cellular effects and mechanisms of glucotoxicity, lipotoxicity and glucolipotoxicity and their dependence on experimental contexts (type of cell line,

species, animal model for ex vivo studies, duration or concentrations of exposures). It should be noted, however, that we observed protection against HFD induced glucose intolerance associated with increased circulating insulin levels in mice with inducible beta-cell specific deletion of DMT-1 (Hansen et al., 2012), providing *in vivo* evidence for the validity of the *in vitro* observations in the present study.

We conclude that iron transport via DMT-1 is a novel central mechanism relaying GLT with generation of hydroxyl radicals from hydrogen peroxide through the Fenton reaction and ROS formation in the cytosolic compartment associated with dissipation of the mitochondrial membrane potential and beta cell apoptosis. Taken together with the accumulating epidemiological evidence suggesting that iron overload leads to diabetes (Bonfils, et al. 2015; Ellervik et al. 2011) and that patients with diabetes have increased tissue iron accumulation (Gabrielsen et al. 2012; Rajpathak, et al. 2009), our findings highlight control of iron levels as an attractive novel treatment option for the prevention of diabetes. Clinical trials are warranted to validate this translation of our preclinical findings.

Declaration of interest

The authors have no conflicts of interest.

Funding

This work was supported by a postdoc grant from Danish Council of Independent Research for JBH.

Acknowledgements

We would like to thank Dr. Nancy C. Andrews for providing the floxed Slc11a2 mice, and Drs. Doug Melton and Palle Serup for the Cre-ERT mice.

References

Arruda AP, Pers BM, Parlakgul G, Guney E, Inouye K & Hotamisligil GS 2014 Chronic enrichment of hepatic endoplasmic reticulum-mitochondria contact leads to mitochondrial dysfunction in obesity. *Nat Med* **20** 1427-1435.

Bedard K & Krause KH 2007 The NOX family of ROS-generating NADPH oxidases: physiology and pathophysiology. *Physiol Rev* **87** 245-313.

Bonfils L, Ellervik C, Friedrich N, Linneberg A, Sandholt CH, Jorgensen ME, Jorgensen T, Hansen T, Pedersen O & Allin KH 2015 Fasting serum levels of ferritin are associated with impaired pancreatic beta cell function and decreased insulin sensitivity: a population-based study. *Diabetologia* **58** 523-533.

Chan CB, De Leo D, Joseph JW, McQuaid TS, Ha XF, Xu F, Tsushima RG, Pennefather PS, Salapatek AM & Wheeler MB 2001 Increased uncoupling protein-2 levels in beta-cells are associated with impaired glucose-stimulated insulin secretion: mechanism of action. *Diabetes* **50** 1302-1310.

Cheng K, Ho K, Stokes R, Scott C, Lau SM, Hawthorne WJ, O'Connell PJ, Loudovaris T, Kay TW, Kulkarni RN, et al. 2010 Hypoxia-inducible factor-1alpha regulates beta cell function in mouse and human islets. *J Clin Invest* **120** 2171-2183.

Coffey R & Knutson MD 2017 The plasma membrane metal-ion transporter ZIP14 contributes to nontransferrin-bound iron uptake by human beta-cells. *Am J Physiol Cell Physiol* **312** C169-C175.

Cooksey RC, Jones D, Gabrielsen S, Huang J, Simcox JA, Luo B, Soesanto Y, Rienhoff H, Abel ED & McClain DA 2010 Dietary iron restriction or iron chelation protects from diabetes and loss of beta-cell function in the obese (ob/ob lep-/-) mouse. *Am J Physiol Endocrinol Metab* **298** E1236-1243.

Cooksey RC, Jouihan HA, Ajioka RS, Hazel MW, Jones DL, Kushner JP & McClain DA 2004 Oxidative stress, beta-cell apoptosis, and decreased insulin secretory capacity in mouse models of hemochromatosis. *Endocrinology* **145** 5305-5312.

Coughlan MT, Thorburn DR, Penfold SA, Laskowski A, Harcourt BE, Sourris KC, Tan AL, Fukami K, Thallas-Bonke V, Nawroth PP, et al. 2009 RAGE-induced cytosolic ROS promote mitochondrial superoxide generation in diabetes. *J Am Soc Nephrol* **20** 742-752.

Cunha DA, Hekerman P, Ladriere L, Bazarra-Castro A, Ortis F, Wakeham MC, Moore F, Rasschaert J, Cardozo AK, Bellomo E, et al. 2008 Initiation and execution of lipotoxic ER stress in pancreatic beta-cells. *J Cell Sci* **121** 2308-2318.

Ehrnstorfer IA, Geertsma ER, Pardon E, Steyaert J & Dutzler R 2014 Crystal structure of a SLC11 (NRAMP) transporter reveals the basis for transition-metal ion transport. *Nat Struct Mol Biol* **21** 990-996.

Ellervik C, Mandrup-Poulsen T, Andersen HU, Tybjaerg-Hansen A, Frandsen M, Birgens H & Nordestgaard BG 2011 Elevated transferrin saturation and risk of diabetes: three population-based studies. *Diabetes Care* **34** 2256-2258.

Ellervik C, Mandrup-Poulsen T, Nordestgaard BG, Larsen LE, Appleyard M, Frandsen M, Petersen P, Schlichting P, Saermark T, Tybjaerg-Hansen A, et al. 2001 Prevalence of hereditary haemochromatosis in late-onset type 1 diabetes mellitus: a retrospective study. *Lancet* **358** 1405-1409.

Ford ES & Cogswell ME 1999 Diabetes and serum ferritin concentration among U.S. adults. *Diabetes Care* **22** 1978-1983.

Friberg J, Tonnesen MF, Heller S, Pociot F, Bodvarsdottir TB & Karlsen AE 2010 Inhibition of the nuclear factor-kappaB pathway prevents beta cell failure and diet induced diabetes in Psammomys obesus. *PLoS One* **5** e13341.

Gabrielsen JS, Gao Y, Simcox JA, Huang J, Thorup D, Jones D, Cooksey RC, Gabrielsen D, Adams TD, Hunt SC, et al. 2012 Adipocyte iron regulates adiponectin and insulin sensitivity. *J Clin Invest* **122** 3529-3540.

Hansen JB, Tonnesen MF, Madsen AN, Hagedorn PH, Friberg J, Grunnet LG, Heller RS, Nielsen AO, Storling J, Baeyens L, et al. 2012 Divalent metal transporter 1 regulates iron-mediated ROS and pancreatic beta cell fate in response to cytokines. *Cell Metab* **16** 449-461.

Jehn M, Clark JM & Guallar E 2004 Serum ferritin and risk of the metabolic syndrome in U.S. adults. *Diabetes Care* **27** 2422-2428.

Jiang R, Manson JE, Meigs JB, Ma J, Rifai N & Hu FB 2004 Body iron stores in relation to risk of type 2 diabetes in apparently healthy women. *JAMA* **291** 711-717.

Jung IR, Choi SE, Jung JG, Lee SA, Han SJ, Kim HJ, Kim DJ, Lee KW & Kang Y 2015 Involvement of iron depletion in palmitate-induced lipotoxicity of beta cells. *Mol Cell Endocrinol* **407** 74-84.

Leloup C, Tourrel-Cuzin C, Magnan C, Karaca M, Castel J, Carneiro L, Colombani AL, Ktorza A, Casteilla L & Penicaud L 2009 Mitochondrial reactive oxygen species are obligatory signals for glucose-induced insulin secretion. *Diabetes* **58** 673-681.

Lenzen S 2017 Chemistry and biology of reactive species with special reference to the antioxidative defence status in pancreatic beta-cells. *Biochim Biophys Acta* **1861** 1929-1942.

Lenzen S, Drinkgern J & Tiedge M 1996 Low antioxidant enzyme gene expression in pancreatic islets compared with various other mouse tissues. *Free Radic Biol Med* **20** 463-466.

Lu JP & Hayashi K 1994 Selective iron deposition in pancreatic islet B cells of transfusional iron-overloaded autopsy cases. *Pathol Int* **44** 194-199.

Lu JP, Hayashi K, Okada S & Awai M 1991 Transferrin receptors and selective iron deposition in pancreatic B cells of iron-overloaded rats. *Acta Pathol Jpn* **41** 647-652.

Maedler K, Schulthess FT, Bielman C, Berney T, Bonny C, Prentki M, Donath MY & Roduit R 2008 Glucose and leptin induce apoptosis in human beta-cells and impair glucose-stimulated insulin secretion through activation of c-Jun N-terminal kinases. *FASEB J* **22** 1905-1913.

Montonen J, Boeing H, Steffen A, Lehmann R, Fritsche A, Joost HG, Schulze MB & Pischon T 2012 Body iron stores and risk of type 2 diabetes: results from the

European Prospective Investigation into Cancer and Nutrition (EPIC)-Potsdam study. *Diabetologia* **55** 2613-2621.
Munoz P, Humeres A, Elgueta C, Kirkwood A, Hidalgo C & Nunez MT 2011 Iron mediates N-methyl-D-aspartate receptor-dependent stimulation of calcium-induced pathways and hippocampal synaptic plasticity. *J Biol Chem* **286** 13382-13392.
Muoio DM & Newgard CB 2008 Mechanisms of disease:Molecular and metabolic mechanisms of insulin resistance and beta-cell failure in type 2 diabetes. *Nat Rev Mol Cell Biol* **9** 193-205.
Nielsen JH 1989 Mechanisms of pancreatic beta-cell growth and regeneration: studies on rat insulinoma cells. *Exp Clin Endocrinol* **93** 277-285.
Prentice KJ, Luu L, Allister EM, Liu Y, Jun LS, Sloop KW, Hardy AB, Wei L, Jia W, Fantus IG, et al. 2014 The furan fatty acid metabolite CMPF is elevated in diabetes and induces beta cell dysfunction. *Cell Metab* **19** 653-666.
Rajpathak SN, Crandall JP, Wylie-Rosett J, Kabat GC, Rohan TE & Hu FB 2009 The role of iron in type 2 diabetes in humans. *Biochim Biophys Acta* **1790** 671-681.
Roma LP, Pascal SM, Duprez J & Jonas JC 2012 Mitochondrial oxidative stress contributes differently to rat pancreatic islet cell apoptosis and insulin secretory defects after prolonged culture in a low non-stimulating glucose concentration. *Diabetologia* **55** 2226-2237.
Thomas C, Mackey MM, Diaz AA & Cox DP 2009 Hydroxyl radical is produced via the Fenton reaction in submitochondrial particles under oxidative stress: implications for diseases associated with iron accumulation. *Redox Rep* **14** 102-108.

Figure Legends

Figure 1. The beta-cell labile iron pool is increased by GLT.

(A) Quantification of the labile iron pool (LIP) from isolated islets of mice fed a high fat diet (HFD) or chow for seven weeks was measured by calcein assay. Means +SEM of n=4-5, *p<0.05, Student's t-test.

(B) Quantification of the LIP from isolated mouse islets exposed to GLT (400 μM palmitate and 30 mM glucose) or vehicle (BSA and ethanol) for up to 72 hours using calcein assay. Means +SEM of 4-7 independent experiments, *p<0.05, Student's t-test.

(C) Quantification of the LIP in human islets exposed to a combination of palmitate (200μM) and oleate (200 μM) for 24 hours using calcein assay. Means +SEM of n=4, *p<0.05, Student's t-test.

(D) Quantification of the LIP in human islets exposed to a combination of IL-1β (150 pg/mL) and IFN-γ (5 ng/mL) for 24 hours using calcein assay. Means +SEM of n=3, *p<0.05, Student's t-test.

(E) Quantification of the LIP in MIN6 cells exposed to with palmitate (400 μM) or vehicle (BSA and ethanol) for up to 72 hours using calcein assay. Means +SEM of 3-4 independent experiments, *p<0.05, Student's t-test.

(F-G) Transferrin (*Trfr*) and divalent metal transporter 1 (*Dmt1*) mRNA in MIN6 cells exposed to palmitate (400 μM) or vehicle (BSA and ethanol) for up to 24 hours. Means +SEM of six independent experiments, *p<0.05, ****p<0.0001, Student's t-test.

Figure 2 GLT induces iron dependent cytosolic ROS production, apoptosis and secretory dysfunction.

(A) Quantification of the LIP from isolated islets treated with different concentrations of DFO using calcein assay. Means +SEM of 4-6 independent experiments.

(B) Apoptosis measurement using DNA-histone complex detection by ELISA in isolated islets exposed to GLT (400 µM palmitate and 30 mM glucose) or vehicle (BSA and ethanol) with or without DFO (0.1 mM) for 48 hours. Means +SEM of four independent experiments, *p<0.05 Control GLT vs. DFO GLT, #p<0.05 Control Vehicle vs. Control GLT, two-way ANOVA.

Cytosolic (C) and mitochondrial (D) thiol oxidation in islets exposed to medium containing 11 mM glucose (G11), G11 supplemented with 400 µM palmitate (G11_PA), 30 mM glucose (G30) or G30 with 400 µM palmitate (G30_PA) with or without DFO (0.1 mM) for 48 hours using cyto-roGFP1 and mito-roGFP1 probes, respectively. Means +SEM of 3-5 independent experiments, **p<0.01 G30_PA vs. G30_PA DFO, Student's t-test.

(E) GSIS from isolated islets exposed to FFA (200 µM palmitate and 200 µM oleate) or vehicle (BSA and ethanol) with or without DFO (0.1 mM) for 48 hours. Means +SEM of four independent experiments, **p<0.01, Student's t-test.

Figure 3 Iron is important for beta-cell mitochondrial function

(A) Quantification of the LIP from isolated islets of inducible beta-cell specific WT ($Cre^{-}Flox^{+}$) or KO ($Cre^{+}Flox^{+}$) mice. Means +SEM of n=5-6 independent experiments, ***p<0.001, Student's t-test.

(B) ROS production in isolated islets of $Cre^{-}Flox^{+}$ and $Cre^{+}Flox^{+}$ islets measured by H_2DCF fluorescence. Means +SEM of n=9, *p<0.05, Student's t-test.

(C) MMP measurements using Rhod123 in isolated $Cre^{-}Flox^{+}$ and $Cre^{+}Flox^{+}$ islets. Left, means +SEM fluorescence traces from islets analyzed, n=8-9. Right, means +SEM AUC of fluorescence traces normalized to time of n=5 independent experiments, *p<0.05, Student's t-test.

Figure 4 Beta-cell specific DMT1 KO reduces GLT mediated apoptosis ROS production and mitochondrial damage.

(A) Apoptosis measurement using DNA-histone complex detection by ELISA in isolated $Cre^{-}Flox^{+}$ and $Cre^{+}Flox^{+}$ islets exposed to GLT (400 µM palmitate and 30 mM glucose) or vehicle (BSA and ethanol). Means +SEM of four independent experiments, **p<0.01, Student's t-test.

(B) ROS production in isolated islets of $Cre^{-}Flox^{+}$ and $Cre^{+}Flox^{+}$ islets exposed to GLT (400 µM palmitate and 30 mM glucose) or vehicle (BSA and ethanol) measured by H_2DCF fluorescence. Means +SEM of three independent experiments, **p<0.01 and **p<0.01 Vehicle $Cre^{-}Flox^{+}$ vs. GLT $Cre^{-}Flox^{+}$, ##p<0.01 GLT $Cre^{-}Flox^{+}$ vs. GLT Cre+Flox+, Student's t-test.

(C) Insulin secretion measured by perifusion in isolated $Cre^{-}Flox^{+}$ and $Cre^{+}Flox^{+}$ islets exposed to GLT (400 µM palmitate and 30 mM glucose) or vehicle (BSA and ethanol). Left panel, perifusion traces. Middle panel, stimulatory index of islet perifusion experiment. Right panel, total islet insulin after perifusion. Graphs show means +SEM of four independent experiments, **p<0.01, Student's t-test.

(D) MMP measurements using Rhod123 in isolated $Cre^{-}Flox^{+}$ islets exposed to GLT (400 µM palmitate and 30mM glucose) or vehicle (BSA and ethanol). Left panel, means +SEM of fluorescence traces from islets analyzed, n=5-7. Right panel, means

+SEM AUC of fluorescence traces normalized to time of n=4-7 independent experiments, *p<0.05, **p<0.01, Student's t-test.

(E) MMP measurements using Rhod123 in isolated $Cre^{+}Flox^{+}$ islet exposed to GLT (400 μM palmitate and 30 mM glucose) or vehicle (BSA and ethanol). Left panel, means +SEM of fluorescence traces from islets analyzed, n=4-5. Right, means +SEM AUC of fluorescence traces normalized to time of n=4-5 independent experiments, *p<0.05, **p<0.01, Student's t-test.

Supplemental figure legends

Figure S1

(A) Quantification of the LIP from isolated islets exposed to palmitate (400 μM) or vehicle (BSA and ethanol) for 24 hours using calcein assay. Means +SEM of three independent experiments, *p<0.05, Student's t-test.

(B) ROS production in MIN6 cells exposed to palmitate (400 μM) or vehicle (BSA and ethanol) for 24 hours measured by H_2DCF fluorescence. Means +SEM of five independent experiments, *p<0.05, Student's t-test.

(C) GSIS in MIN6 cells exposed to palmitate (400 μM) or vehicle (BSA and ethanol) for 24 hours. Means +SEM of six independent experiments, *p<0.05, Student's t-test.

(D) Apoptosis measurement using DNA-histone complex detection by ELISA in MIN6 cells exposed to palmitate (400 μM) or vehicle (BSA and ethanol) for 24 hours. Means +SEM of five independent experiments, **p<0.01, Student's t-test.

(E-I) Expression of ferritin heavy chain (*Fth*), ferritin light chain (*Ftl*) ferroportin (*Fpn*) pancreatic duodenum homeobox (*Pdx*) 1, and insulin (*Ins*) 1 mRNA in MIN6 cells exposed to palmitate (400 μM) or vehicle (BSA and ethanol) for up to 24 hours. Means +SEM of six independent experiments, *p<0.05, Student's t-test.

Figure S2

(A) Stimulatory index (fold of 3 mM glucose, right) of mouse islets exposed to various concentrations of DFO for 48 hours. Means +SEM of five independent experiments.

(B) Quantification of accumulated insulin secreted into the media from isolated islets during treatment with DFO (0.1mM) for 48 hours. Means +SEM of three independent experiments.
(C) Total islet insulin content of islets after treatment with DFO (0.1 mM) for 48 hours. Means +SEM of three independent experiments.
(D) Quantification of LIP in MIN6 cells exposed to palmitate (400 μM) with increasing concentrations of DFO. Data shown as fold of vehicle control with means +SEM of 3-4 independent experiments, *$p<0.05$, Student's t-test.

Figure S3

(A) DMT1 KO verification by RT-PCR in isolated $Cre^{-}Flox^{+}$ and $Cre^{+}Flox^{+}$ islets. Means +SEM of n=2 independent experiments.
(B) GSIS and KCl induced insulin secretion from isolated $Cre^{-}Flox^{+}$ and $Cre^{+}Flox^{+}$ islets normalized to secretion at 3 mM glucose. Means +SEM of three independent experiments.

Figure S4

(A-C) Measurements of IL-6, TNF-α and MCP-1 secretion to the culture medium from islets exposed to GLT (400 μM palmitate and 30 mM glucose) or vehicle (BSA and ethanol) in the presence or absence of DFO (0.1 mM) for 48 hours, or (D-F) in GLT or vehicle exposed $Cre^{-}Flox^{+}$ and $Cre^{+}Flox^{+}$ islets. Means +SEM of 2-4 independent experiments, *$p<0.05$, Student's t-test.

Figure 1

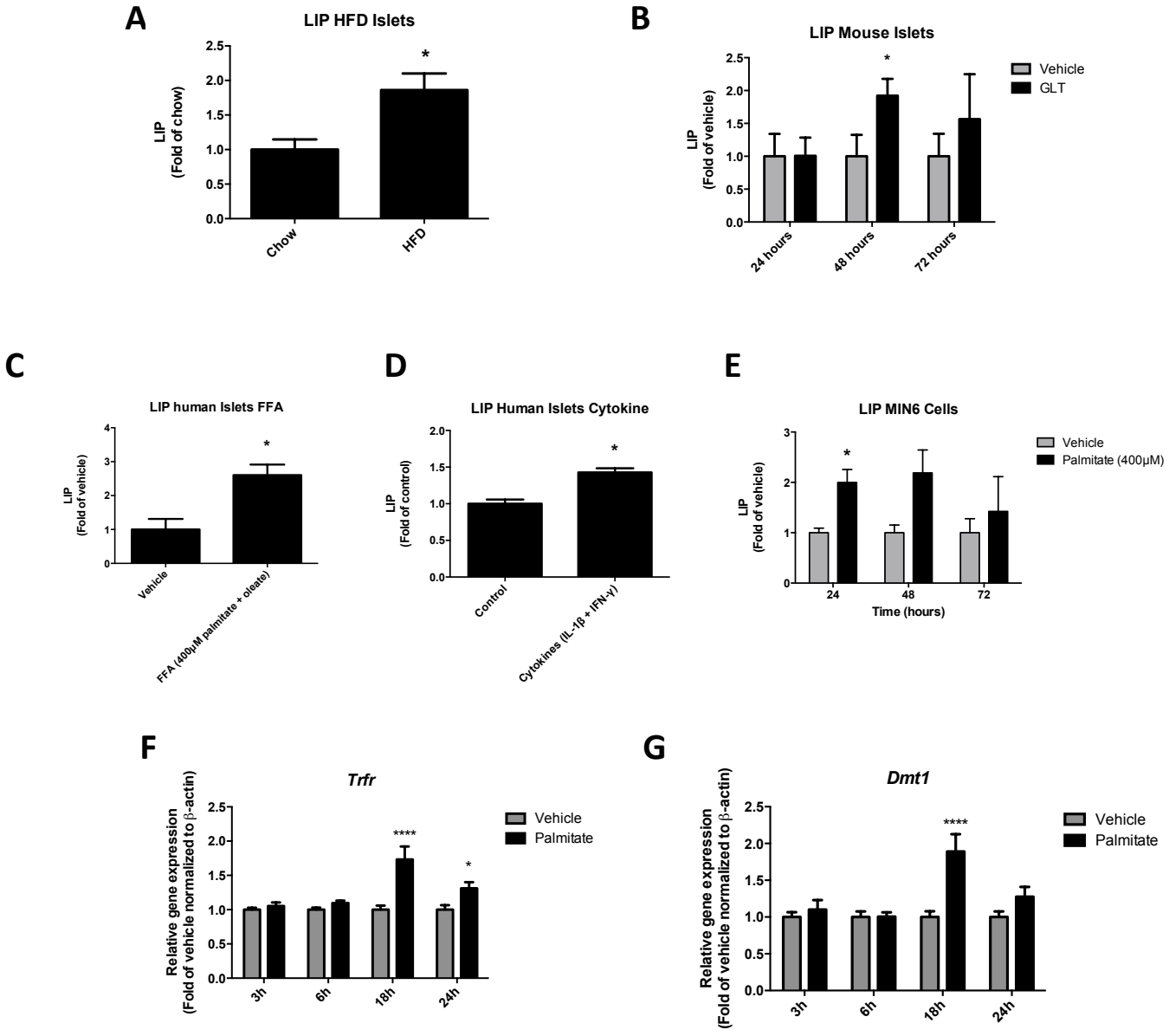
A
LIP HFD Islets
LIP (Fold of chow)
Chow
HFD
B
LIP Mouse Islets
LIP (Fold of vehicle)
Vehicle
GLT
24 hours
48 hours
72 hours
C
LIP human Islets FFA
LIP (Fold of vehicle)
Vehicle
FFA (400µM palmitate + oleate)
D
LIP Human Islets Cytokine
LIP (Fold of control)
Control
Cytokines (IL-1β + IFN-γ)
E
LIP MIN6 Cells
LIP (Fold of vehicle)
Vehicle
Palmitate (400µM)
Time (hours)
F
Trfr
Relative gene expression (Fold of vehicle normalized to β-actin)
Vehicle
Palmitate
3h
6h
18h
24h
G
Dmt1
Relative gene expression (Fold of vehicle normalized to β-actin)
Vehicle
Palmitate
3h
6h
18h
24h

Figure 2

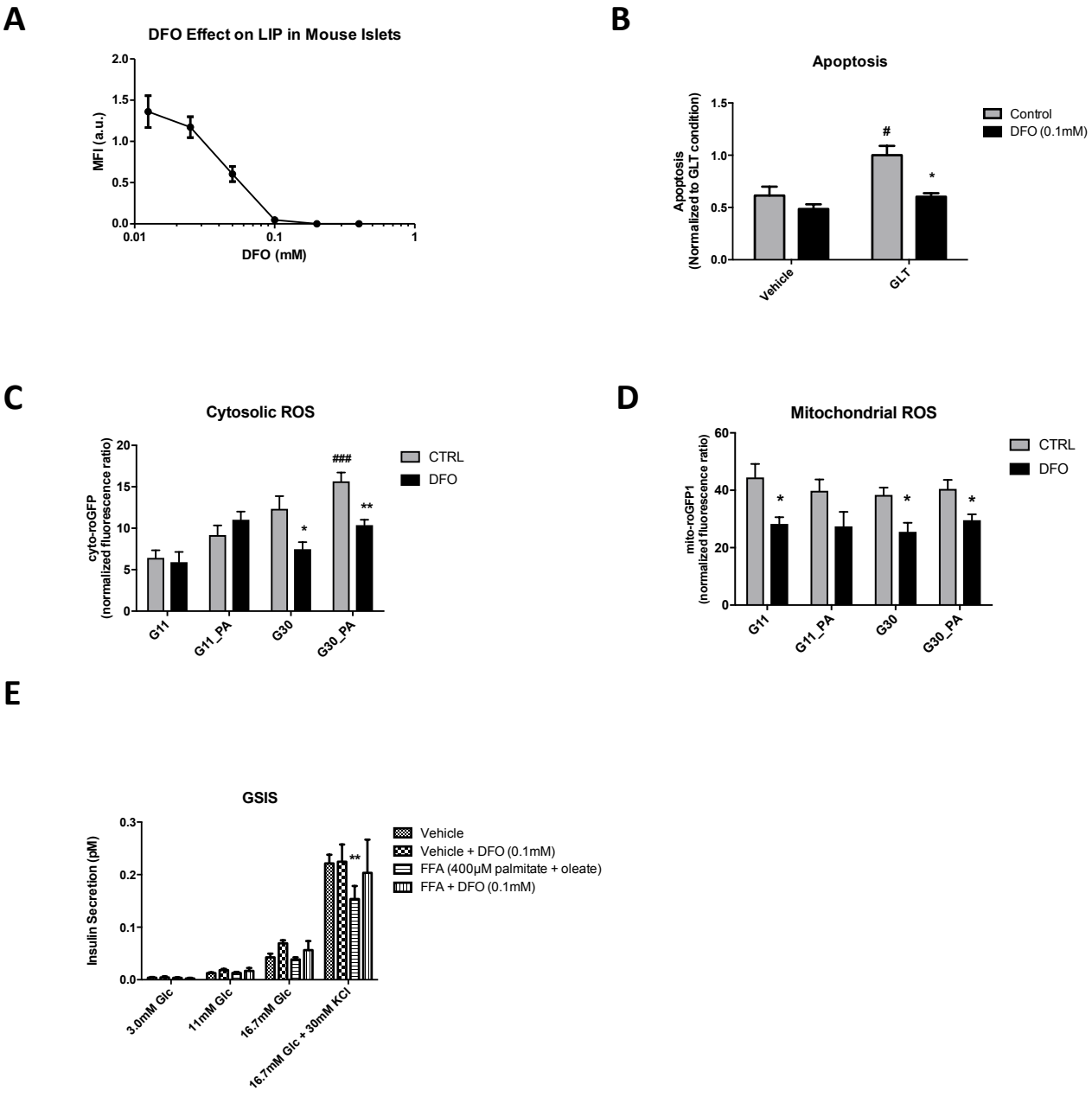
A
DFO Effect on LIP in Mouse Islets
MFI (a.u.)
DFO (mM)
B
Apoptosis
Apoptosis (Normalized to GLT condition)
Control
DFO (0.1mM)
Vehicle
GLT
C
Cytosolic ROS
cyto-roGFP (normalized fluorescence ratio)
CTRL
DFO
G11
G11_PA
G30
G30_PA
D
Mitochondrial ROS
mito-roGFP1 (normalized fluorescence ratio)
CTRL
DFO
G11
G11_PA
G30
G30_PA
E
GSIS
Insulin Secretion (pM)
Vehicle
Vehicle + DFO (0.1mM)
FFA (400μM palmitate + oleate)
FFA + DFO (0.1mM)
3.0mM Glc
11mM Glc
16.7mM Glc
16.7mM Glc + 30mM KCl

Figure 3

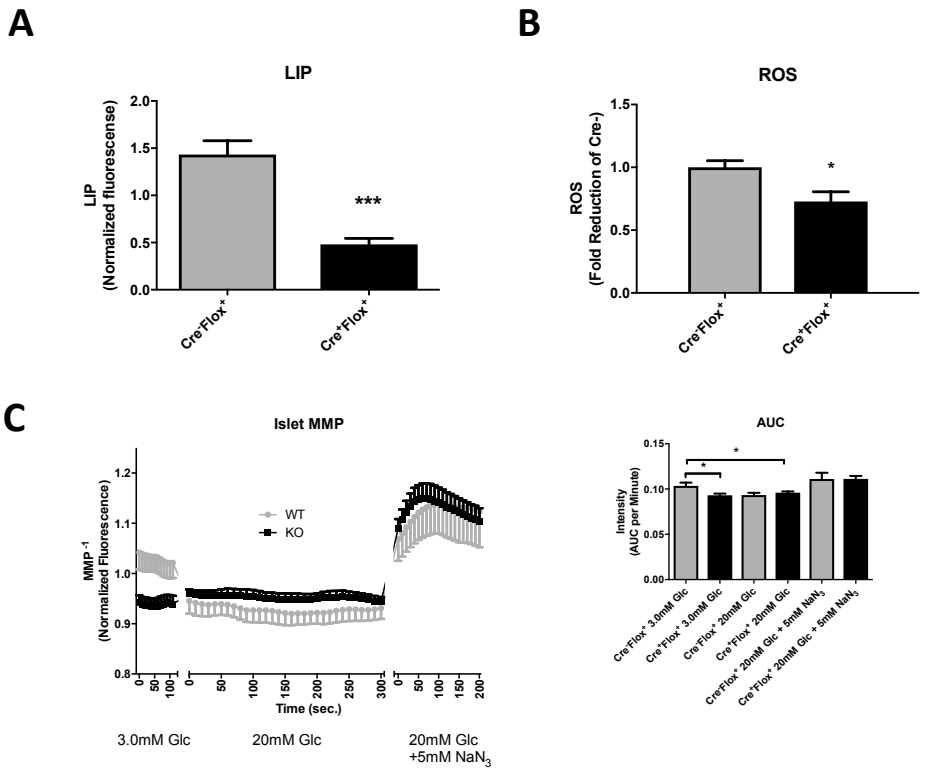
A
LIP
LIP (Normalized fluorescense)
2.0
1.5
1.0
0.5
0.0
***
Cre-Flox+
Cre+Flox+
B
ROS
ROS (Fold Reduction of Cre-)
1.5
1.0
0.5
0.0
*
Cre-Flox+
Cre+Flox+
C
Islet MMP
MMP-1 (Normalized Fluorescence)
1.2
1.1
1.0
0.9
0.8
WT
KO
0
50
100
0
50
100
150
200
250
300
0
50
100
150
200
Time (sec.)
3.0mM Glc
20mM Glc
20mM Glc +5mM NaN3
AUC
Intensity (AUC per Minute)
0.15
0.10
0.05
0.00
*
*
Cre-Flox+ 3.0mM Glc
Cre+Flox+ 3.0mM Glc
Cre-Flox+ 20mM Glc
Cre+Flox+ 20mM Glc
Cre-Flox+ 20mM Glc + 5mM NaN3
Cre+Flox+ 20mM Glc + 5mM NaN3

Figure 4

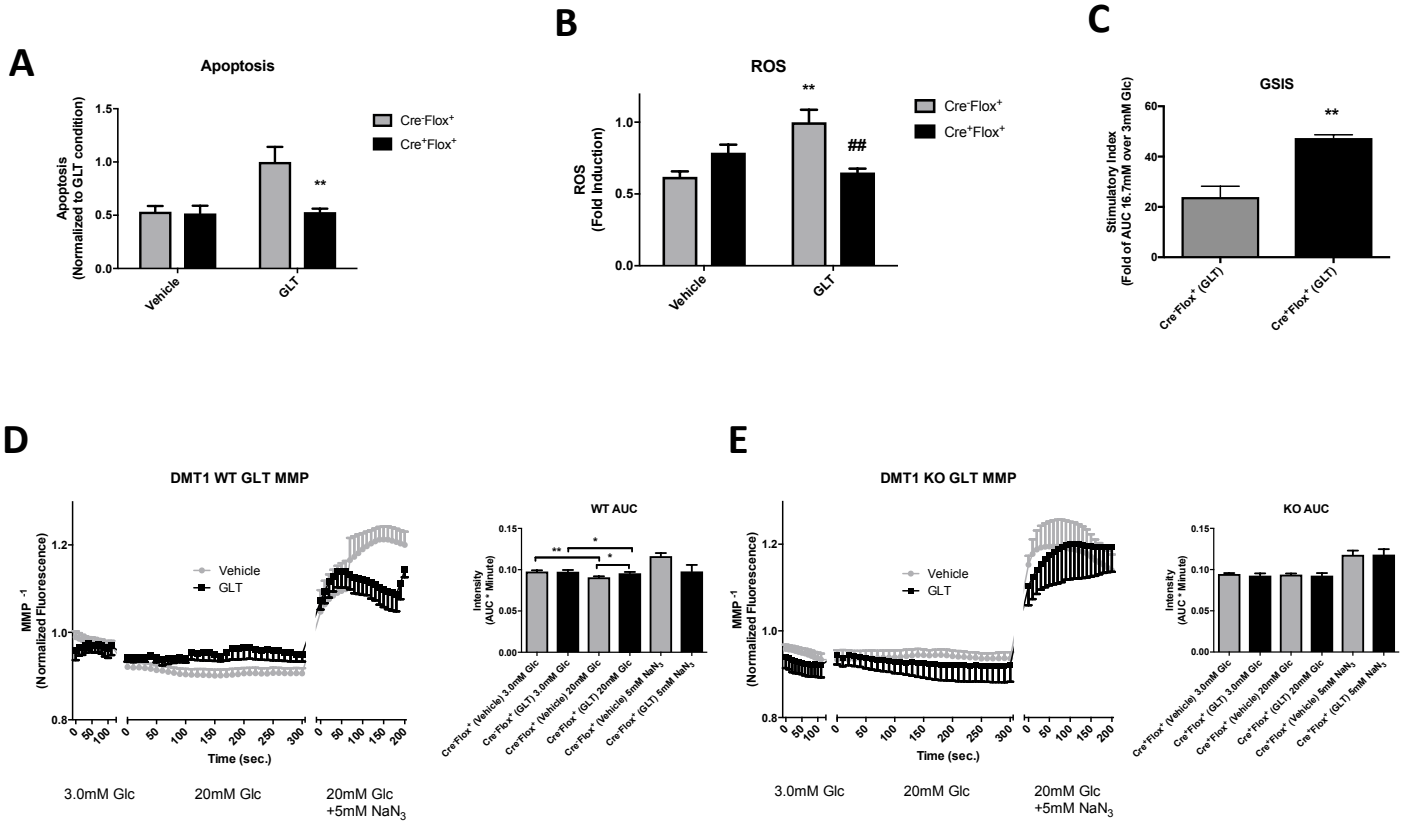
A
Apoptosis
Apoptosis (Normalized to GLT condition)
Cre-Flox+
Cre+Flox+
Vehicle
GLT
**
B
ROS
ROS (Fold Induction)
**
##
C
GSIS
Stimulatory Index (Fold of AUC 16.7mM over 3mM Glc)
**
Cre-Flox+ (GLT)
Cre+Flox+ (GLT)
D
DMT1 WT GLT MMP
MMP -1 (Normalized Fluorescence)
Vehicle
GLT
Time (sec.)
3.0mM Glc
20mM Glc
20mM Glc +5mM NaN3
WT AUC
Intensity (AUC * Minute)
E
DMT1 KO GLT MMP
KO AUC

Figure S1

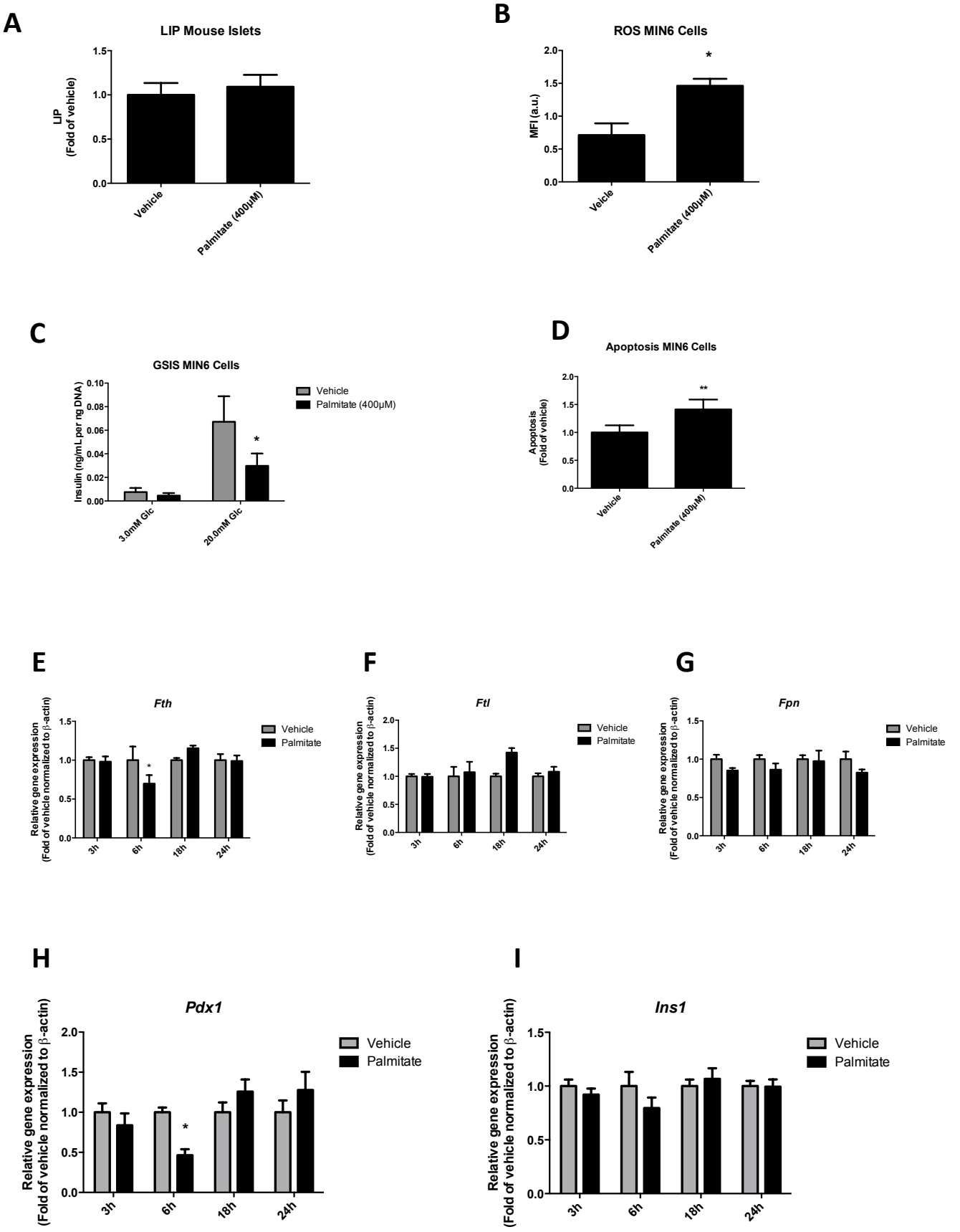
A
LIP Mouse Islets
LIP (Fold of vehicle)
1.5
1.0
0.5
0.0
Vehicle
Palmitate (400μM)
B
ROS MIN6 Cells
MFI (a.u.)
2.0
1.5
1.0
0.5
0.0
*
Veicle
Palmitate (400μM)
C
GSIS MIN6 Cells
Insulin (ng/mL per ng DNA)
0.10
0.08
0.06
0.04
0.02
0.00
*
3.0mM Glc
20.0mM Glc
Vehicle
Palmitate (400μM)
D
Apoptosis MIN6 Cells
Apoptosis (Fold of vehicle)
2.0
1.5
1.0
0.5
0.0
**
Vehicle
Palmitate (400μM)
E
Fth
Relative gene expression (Fold of vehicle normalized to β-actin)
1.5
1.0
0.5
0.0
*
3h
6h
18h
24h
Vehicle
Palmitate
F
Ftl
Relative gene expression (Fold of vehicle normalized to β-actin)
2.0
1.5
1.0
0.5
0.0
3h
6h
18h
24h
Vehicle
Palmitate
G
Fpn
Relative gene expression (Fold of vehicle normalized to β-actin)
1.5
1.0
0.5
0.0
3h
6h
18h
24h
Vehicle
Palmitate
H
Pdx1
Relative gene expression (Fold of vehicle normalized to β-actin)
2.0
1.5
1.0
0.5
0.0
*
3h
6h
18h
24h
Vehicle
Palmitate
I
Ins1
Relative gene expression (Fold of vehicle normalized to β-actin)
1.5
1.0
0.5
0.0
3h
6h
18h
24h
Vehicle
Palmitate

Figure S2

A

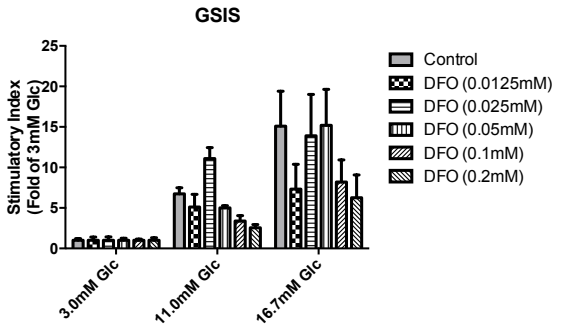

B

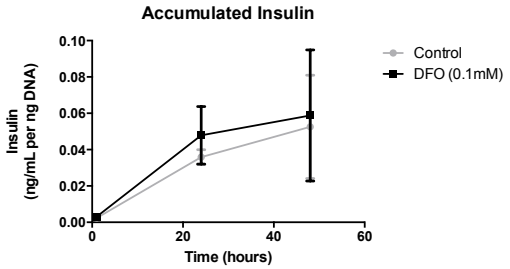

C

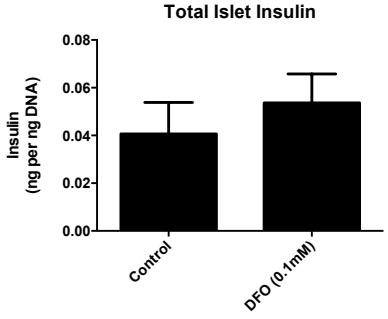

D

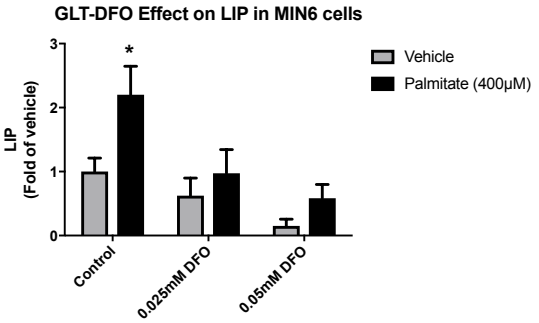

Figure S3

A

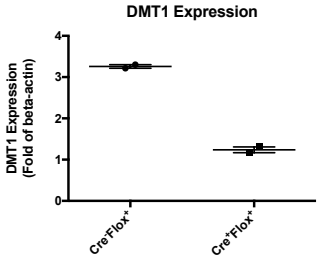
DMT1 Expression
DMT1 Expression
(Fold of beta-actin)
4
3
2
1
0
Cre-Flox+
Cre+Flox+

B

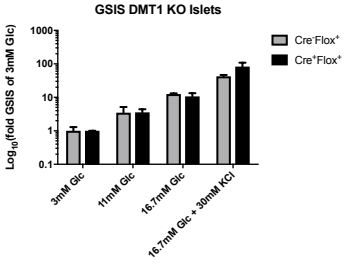
GSIS DMT1 KO Islets
Log10(fold GSIS of 3mM Glc)
1000
100
10
1
0.1
Cre-Flox+
Cre+Flox+
3mM Glc
11mM Glc
16.7mM Glc
16.7mM Glc + 30mM KCl

Figure S4

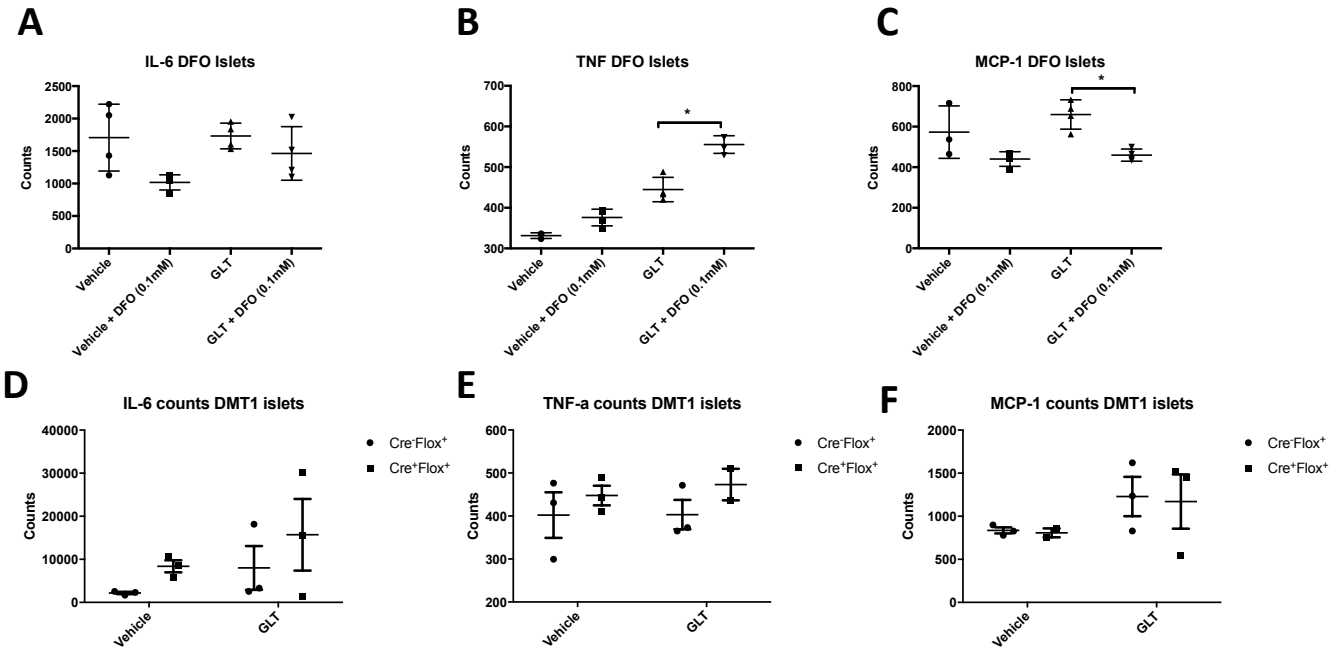
A
IL-6 DFO Islets
Counts
2500
2000
1500
1000
500
0
Vehicle
Vehicle + DFO (0.1mM)
GLT
GLT + DFO (0.1mM)
B
TNF DFO Islets
Counts
700
600
500
400
300
*
Vehicle
Vehicle + DFO (0.1mM)
GLT
GLT + DFO (0.1mM)
C
MCP-1 DFO Islets
Counts
800
600
400
200
0
*
Vehicle
Vehicle + DFO (0.1mM)
GLT
GLT + DFO (0.1mM)
D
IL-6 counts DMT1 islets
Counts
40000
30000
20000
10000
0
Vehicle
GLT
Cre-Flox+
Cre+Flox+
E
TNF-a counts DMT1 islets
Counts
600
500
400
300
200
Vehicle
GLT
Cre-Flox+
Cre+Flox+
F
MCP-1 counts DMT1 islets
Counts
2000
1500
1000
500
0
Vehicle
GLT
Cre-Flox+
Cre+Flox+

Supplemental Information

Supplemental Materials and Methods

Animal care

The floxed *Slc11a2* (Gunshin et al., 2005) and *Cre-ERT* (Gu et al., 2002) mice were bred by heterozygous breeding to generate the inducible beta-cell specific DMT1 knock-out (KO) mouse (Hansen et al., 2012), used for experimentation at 10-12 weeks of age. Tamoxifen-induced beta-cell specific DMT1 KO was performed as previously described (Hansen et al., 2012). CD1 and NMRI mice were used for wild-type mouse experiments. For high fat diet (HFD) studies, five-week-old male CD1 mice were purchased from Charles River (Toronto, ON, Canada) and allowed to acclimatize for one week prior to being placed on a high fat diet with 60% kcal from fat (OpenSource diets D12492, Research Diets Inc, New Brunswick, NJ, USA) or a matched sucrose chow diet with 10% kcal from fat (OpenSource diets D12450J, Research Diets Inc, New Brunswick, NJ, USA) for eight weeks.

Islet Isolation

Mice were sacrificed by cervical dislocation, and pancreata were inflated with 0.8 mg/mL collagenase V (Sigma, Brøndby, Denmark) solution in RPMI 1640 (Gibco, Nærum, Denmark) without serum via injection through the common bile duct. Digestion was carried out on a 37°C water bath, and the enzymatic reaction was stopped by addition of cold RMPI 1640 supplemented with 10% foetal bovine serum (FBS, Gibco, Nærum, Denmark) and 0.1% penicillin and streptomycin. Islets were hand-picked and cultured over night before experimentation.

Islet and cell culture reagents

The iron chelator desferroxamine (DFO) (Sigma, Brøndby, Denmark) was dissolved in ultra-pure water and sterile filtered. DFO was prepared fresh for each experiment. The cell permeant iron chelator deferasirox (D-sirox) (Santa Cruz Biotechnology, Heidelberg, Germany) was diluted in DMSO.
IL-1β (Invitrogen, Nærum, Denmark) and IFN-γ (RnD Systems, Abingdon, UK) stocks were prepared in PBS (Gibco, Nærum, Denmark) supplemented with 0.1%

fatty acid-free bovine serum albumin (BSA) (Sigma, Brøndby, Denmark) as carrier protein.

Calcein assay

Islets were incubated in freshly made imaging buffer (130 mM NaCl, 5 mM KCl, 2 mM $CaCl_2$, 1 mM $MgCl_2$, 5 mM $NaHCO_3$, 10 mM HEPES, pH = 7.4) with 0.25 μM calcein-AM (Molecular Probes, Nærum, Denmark) for 1 hour. Fluorescence (excitation: 488 nm, emission: 517 nm) was detected using an Olympus BX51W1 microscope (Tokyo, Japan) with a ×20/0.95NA water immersion objective and a cooled charge-coupled device camera and analyzed using ImageMaster version 3.0 software (Photon Technology International, Birmingham, NJ, USA) or Flex Station 3 (Molecular Devices, Sunnyvale, CA, USA) in black clear-bottom 96-well plates. Total islet calcein loading was measured after chelation with 0.015 mM D-Sirox, and changes in LIP was measured as difference between total calcein load and quenched calcein fluorescence.

Mitochondrial membrane potential

Islets were grown on extracellular matrix-coated coverslips (Biological Industries, Kibbutz Beit-Haemek, Israel) in RPMI 1640 supplemented with 2% human serum (BioWhittaker, VWR, Søborg, Denmark) until attached. Islets were cultured in RPMI 1640 with 10% FBS for 48 hours prior to experimentation or treated with vehicle or GLT. Two hours prior to experimentation, islets were cultured in 3.0 mM glucose RPMI to establish basal mitochondrial membrane potential. Islets were loaded with Rhodamine123 (Rhod123; Molecular Probes, Nærum, Denmark) (2.5 mg/mL) for 10 min in imaging buffer and the increase in mitochondrial membrane potential upon increase in glucose concentration (3 mM to 20 mM) was measured as quenching of Rhod123 fluorescence. At the end of experiment, total depolarization of the mitochondrial membrane was measured after addition of 5 mM NaN_3 (Sigma, Denmark). Fluorescence was recorded using upright Zeiss (Zeiss, Oberkochen, Germany) LSM 700 confocal microscope with a 488 nm 10 mV diode laser, x40/0.75W N-Achroplan water immersion objective, and full pinhole. Data was analyzed using Zeiss Black 2012 (Zeiss, Oberkochen, Germany) and Image J (Fiji).

Primers

Fpn: Fwd: 5' GCTGCTAGAATCGGTCTTTGG '3; Rev: 5' CAGCAACTGTGTCACCGTCAA '3. *Trfr*: Fwd: 5' GAGGAACCAGACCGTTTAGTTGT '3; Rev: 5' CTTCGCCGCAACACCAGCA '3. *Ftl*: Fwd: 5' TGGCCATGGAGAAGAACCTGAATC '3; Rev: 5' GGCTTTCCAGGAAGTCACAGAGAT '3. *Fth*: Fwd: 5' TCAGTCACTACTGGAACTGC '3; Rev: 5' CGTGGTCACCCAGTTCTTTA '3. *Pdx1*: Fwd: 5' ACAAATACATCTCCCGGCCC '3; Rev: 5' GTCACCGCACAATCTTGCTC '3. Beta-Actin: Fwd: 5' CTGAATGGCCCAGGTCTGA '3; Rev: 5' CCCTGGCTGCCTCAACAC '3. *Ins1*: Fwd: 5' GGTGGGCATCCAGTAACCCCCA '3; Rev: 5'GAAGCCACGCTCCCCACACA '3. *Dmt1*: Fwd: 5'CGGAGTCCTCATCACCATCG '3; Rev: 5' TGGGCTTCACTGTAATGTACTCA '3.

ROS

Twenty-five islets per condition in duplicates were used for ROS detection using CM-H2DCFDA (Molecular Probes, Nærum, Denmark). Islets were loaded with CM-H2DCFDA (10 μM) for 45 minutes in imaging buffer, washed once and ROS was detected on Flex Station 3 (Molecular Devices, Sunnyvale, CA, USA), with a repeated measurement after 45 minutes (Friberg et al., 2010).

Quantification of cytosolic and mitochondrial thiol oxidation

Isolated islets were cultured overnight in serum-free RPMI medium supplemented with 5g/L BSA. Islets were dispersed by incubation in trypsin for 3 min, and the reaction was stopped with RPMI medium supplemented with 10% FBS. The islets were then cultured, in batches of 10, at different glucose concentrations and/or palmitate with or without DFO (0.1 mM).

Islets were infected with 200 MOI of an *adenovirus* coding mito-roGFP1 or cyto-roGFP1. Two days later, they were transferred to a 37°C temperature-controlled perifusion chamber placed on the stage of an inverted microscope. Islets were perifused at a flow rate of 1 ml/min with a bicarbonate-buffered Krebs solution containing the same glucose concentration as during previous culture. Cell fluorescence was measured at 535 nm during alternate excitation at 400/480 nm every 30 s. After 20 min of perifusion in Krebs, 10 mM DTT was added to

maximally reduce roGFP1, followed by 100 μM aldrithiol to maximally oxidize roGPF. The fluorescence ratio during the initial perifusion period was normalized to the ratio in DTT (set to 0%) and in aldrithiol (set to 100%).

Transcription factor binding site prediction

Prediction of transcription factor binding sites was performed at Sabiosiences homepage (http://www.sabiosciences.com/chipqpcrsearch.php)

Supplemental references

Gu, G., Dubauskaite, J., and Melton, D.A. (2002). Direct evidence for the pancreatic lineage: NGN3+ cells are islet progenitors and are distinct from duct progenitors. Development *129*, 2447-2457.

Gunshin, H., Fujiwara, Y., Custodio, A.O., Direnzo, C., Robine, S., and Andrews, N.C. (2005). Slc11a2 is required for intestinal iron absorption and erythropoiesis but dispensable in placenta and liver. The Journal of Clinical Investigation *115*, 1258-1266.

Hansen, J.B., Tonnesen, M.F., Madsen, A.N., Hagedorn, P.H., Friberg, J., Grunnet, L.G., Heller, R.S., Nielsen, A.O., Storling, J., Baeyens, L., et al. (2012). Divalent metal transporter 1 regulates iron-mediated ROS and pancreatic beta cell fate in response to cytokines. Cell Metabolism *16*, 449-461.